Forum Original Research Communication

Metallothionein Attenuates 3-Morpholinosydnonimine (SIN-1)-Induced Oxidative Stress in Dopaminergic Neurons

SUSHIL K. SHARMA and MANUCHAIR EBADI

ABSTRACT

Parkinson's disease is characterized by a progressive loss of dopaminergic neurons in the substantia nigra zona compacta, and in other subcortical nuclei associated with a widespread occurrence of Lewy bodies. The causes of cell death in Parkinson's disease are still poorly understood, but a defect in mitochondrial oxidative phosphorylation and enhanced oxidative stress have been proposed. We have examined 3-morpholinosydnon-imine (SIN-1)-induced apoptosis in control and metallothionein-overexpressing dopaminergic neurons, with a primary objective to determine the neuroprotective potential of metallothionein against peroxynitrite-induced neurodegeneration in Parkinson's disease. SIN-1 induced lipid peroxidation and triggered plasma membrane blebbing. In addition, it caused DNA fragmentation, α-synuclein induction, and intramitochon-drial accumulation of metal ions (copper, iron, zinc, and calcium), and enhanced the synthesis of 8-hydroxy-2-deoxyguanosine. Furthermore, it down-regulated the expression of Bcl-2 and poly(ADP-ribose) polymerase, but up-regulated the expression of caspase-3 and Bax in dopaminergic (SK-N-SH) neurons. SIN-1 induced apoptosis in aging mitochondrial genome knockout cells, α-synuclein-transfected cells, metallothionein dou-ble-knockout cells, and caspase-3-overexpressed dopaminergic neurons. SIN-1-induced changes were attenu-ated with selegiline or in metallothionein-transgenic striatal fetal stem cells. SIN-1-induced oxidation of dopa-mine to dihydroxyphenylacetaldehyde was attenuated in metallothionein-transgenic fetal stem cells and in cells transfected with a mitochondrial genome, and enhanced in aging mitochondrial genome knockout cells, in metallothionein double-knockout cells and caspase-3 gene-overexpressing dopaminergic neurons. Selegi-line, melatonin, ubiquinone, and metallothionein suppressed SIN-1-induced down-regulation of a mitochon-drial genome and up-regulation of caspase-3 as determined by reverse transcription–polymerase chain reac-tion. The synthesis of mitochondrial 8-hydroxy-2-deoxyguanosine and apoptosis-inducing factors were increased following exposure to 1-methyl-4-phenylpyridinium ion or rotenone. Pretreatment with selegiline or metal-lothionein suppressed 1-methyl-4-phenylpyridinium ion-, 6-hydroxydopamine-, and rotenone-induced increases in mitochondrial 8-hydroxy-2-deoxyguanosine accumulation. Transfection of aging mitochondrial genome knockout neurons with mitochondrial genome encoding complex-1 or melanin attenuated the SIN-1-induced increase in lipid peroxidation. SIN-1 induced the expression of α-synuclein, caspase-3, and 8-hydroxy-2-deoxyguanosine, and augmented protein nitration. These effects were attenuated by metallothionein gene overexpression. These studies provide evidence that nitric oxide synthase activation and peroxynitrite ion overproduction may be involved in the etiopathogenesis of Parkinson's disease, and that metallothionein gene induction may provide neuroprotection. *Antioxid. Redox Signal.* 5, 251–264.

Department of Pharmacology, Physiology, and Therapeutics, University of North Dakota School of Medicine and Health Sciences, Grand Forks, ND, U.S.A.

INTRODUCTION

Althrough the exact etiopathogenesis of Parkinson's disease (PD) remains unknown, it has been hypothesized that the neuronal demise of nigrostriatal dopaminergic neurons (DA neurons) could occur due to the production of endogenous neurotoxins, such as tetrahydroisoquinolines, or by exposure to various environmental neurotoxins, such as rotenone (15). These neurotoxins produce a significant downregulation of mitochondrial complex-1 (ubiquinone NADH-oxidoreductase), as observed in the majority of PD patients. Furthermore, significantly reduced glutathione in the substantia nigra (SN) enhances the risk of free radical [mainly hydroxyl ($\cdot$OH) and nitric oxide ($\cdot$NO)] overproduction, leading to neuronal damage in PD.

NO plays a critical role in mediating neurotoxicity associated with various neurological disorders, such as stroke, PD, HIV dementia (1, 5, 9, 16, 20), and multiple sclerosis (50). In the SN of PD patients, a significant increase in the density of glial cells expressing tumor necrosis factor-α, interleukin-1β, and interferon-γ has been observed. Although CD23 was not detectable in the SN of control subjects, it was found in both astroglial and microglial cells of parkinsonian patients, indicating the existence of cytokine/CD23-dependent activation pathways of inducible NO synthase (iNOS) and of proinflammatory mediators in glial cells and their involvement in the pathophysiology of PD (21). In addition to NO, accumulation of iron in the SN has been implicated in the death of DA neurons in PD (55, 56). Peroxynitrite (ONOO$^-$) ions, generated in the mitochondria by Ca^{2+}-dependent NO synthase (NOS) activation during oxidative- and nitrative stress, readily react with lipids, aromatic amino- acids, or metalloproteins, inhibiting mitochondrial respiratory complexes, and hence are thought to be involved in the etiopathogenesis of many diseases, including PD (52).

Although NO has been shown to possess both apoptogenic and apoptostatic properties, its overproduction during oxidative and nitrative stresses could induce deleterious consequences on mitochondrial complex-1 activity (6, 17). We have discovered recently that metallothionein (MT) gene overexpression in MT transgenic (MT_{trans}) mouse brain inhibited the 1-methyl-4-phenyl-1,23,6-tetrahydropyridine(MPTP)-induced nitration of α-synuclein (α-Syn), and preserved mitochondrial coenzyme Q_{10} levels, affording neuroprotection against nitrative and oxidative stress of aging brain (48, 49). In addition, MT isoforms are able to suppress 6-hydroxy-dopamine (6-OHDA)-induced $\cdot$OH radical generation (48). We have also reported that selegiline, a monoamine oxidase B inhibitor, provides neuroprotection via MT gene overexpression (14).

As the involvement of oxidative and nitrative stresses is now advocated in the etiopathogenesis of PD (1, 5, 9, 16, 20), a detailed study was needed to explore the exact molecular mechanism of NO-mediated neurodegeneration and MT-induced neuroprotection in PD. 3-Morpholinosydnonimine (SIN-1), a vasorelaxant, a soluble guanylyl cyclase stimulator, and a potent ONOO$^-$ generator, produced not only oxidative, but also nitrative stresses in DA neurons, portending to play an important role in understanding the exact etiopathogenesis of PD (6). Therefore, we have investigated the extent of neuroprotection afforded by MT against SIN-1-induced lipid peroxida-

tion, caspase-3 activation, and mitochondrial 8-hydroxy-2-deoxyguanosine (8-OH-2dG) synthesis in human DA (SK-N-SH) cell line, and in MT-overexpressed striatal DA neurons. These studies have shown that selegiline affords neuroprotection by enhancing MT gene expression and by down-regulating α-Syn expression, a Lewy body molecular marker. MT pretreatment also attenuated SIN-1-induced intramitochondrial accumulation of metal ions (Cu^{2+}, Fe^{3+}, and Ca^{2+}), known to be involved in the etiopathogeneis of PD, suggesting a possible neuroprotective potential for MT gene overexpression in attenuating neurotoxin-induced parkinsonism.

MATERIALS AND METHODS

Chemicals

Cell culture materials, including powdered Dulbecco's modified Eagle medium (DMEM), fetal bovine serum, streptopenicillin, Ham's F-12 medium, trypsin, and specific primers for reverse transcription–polymerase chain reaction (RT-PCR) were purchased from GibcoBRL Life Technologies (Rockville, MD, U.S.A.). First-strand cDNA kit was purchased from Stratagene (La Jolla, CA, U.S.A.). Mouse anti-MT antibody was purchased from Zymed Laboratories (San Francisco CA, U.S.A.). Anti-α-Syn antibody, apoptosis-inducing factor (AIF), and anti-nitrotyrosine polyclonal antibodies were purchased from Chemicon International Inc. (Temecula, CA, U.S.A.). Caspase-3 assay kit was purchased from Pharmingen, Becton–Dickinson (Palo Alto, CA, U.S.A.). [^{35}S]Methionine was purchased from NEN Dupont (Boston, MA, U.S.A.). ATP-Lite™ kit was purchased from Packard (Meriden, CT, U.S.A.). Vector (pEGFP-N1) was purchased from BD Bioscience Clontech (Palo Alto, CA, U.S.A.). Liposome-based Effectine Transfection reagent with DNA enhancer was purchased from Qiagen Inc. (Stanford, CA, U.S.A.). Protein assay dye was purchased from Bio-Rad Laboratories (Hercules, CA, U.S.A.). ECL chemiluminescence kit and nitrocellulose membranes were purchased from Amersham Bioscience Corp. (Piscataway, NJ, U.S.A.). Mitochondrial membrane potential ($\Delta\Psi$) fluorochrome, 5,5′,6,6′-tetrachloro-1,1′,3,3′-tetraethyl-benzimidazolocarbocyanide iodide (JC-1), nucleocytoplasmic fluorochromes, 4′,6-diamidino-2-phenylindole dihydrochloride (DAPI), ethidium bromide, acridine orange, and fluorescein isothiocyanate (FITC)-conjugated antimouse IgG were purchased from Molecular Probes (Eugene, OR, U.S.A.). All other chemicals were of reagent grade quality and were purchased from Sigma Chemical Company (St. Louis, MO, U.S.A.).

Experimental animals

Experimental animals were housed in temperature- and humidity-controlled rooms with a 12-h day and 12-h night cycle and were provided with commercially prepared chow and water *ad libitum*. The animals were acclimated to laboratory conditions for at least 4 days prior to experimentation. Care was also taken to avoid any distress to animals during the period of experiment. Breeder pairs of control wild-type (control$_{wt}$) C57BJ6, MT double knockout (MT_{dko}), and MT_{trans} mice weighing 25–30 g were purchased from Jackson's Laboratories (Minneapolis, MN, U.S.A.). The animals were main-

tained in an air-conditioned animal house facility in hepta-filtered cages with free access to water and lab chow. The zinc, copper, and iron contents in the lab chow were monitored by an atomic absorption spectrophotometer to maintain their adequate supply.

Preparation of fetal stem cells

Pregnant female mice from different genotypes were anesthetized with tribromoethane (350 mg/kg, i.p) on the 18th day of gestation. The developing embryos were removed from the womb by cesarean section under strictly sterilized conditions. The embryos were washed three times in Dulbecco's phosphate-buffered saline (d-PBS; pH 4.5, 0.15 M) and anesthetized over dry ice before decapitation. The scalp was removed, and different brain regions were isolated using a stereobinocular dissecting microscope.

Fetal brain regions (hippocampus, SN, striatum, and cerebellum) dissected from the 18-day-old mouse fetuses were placed in 0.1% Trypsin solution containing Ca^{2+} and Mg^{2+}-free Hanks' balanced salt solution (HBSS) buffered to pH 7.3 with 10 mM HEPES. The tissues were incubated for 15 min at 37°C and then washed three times with HBSS. The tissues were resuspended in ~1 ml of HBSS, and the cells were dissociated by passage through a series of Pasteur pipettes with flame-narrowed tips.

The culture dish (size 35 mm) was precoated with a solution of 0.01% polylysine hydrobromide in borate buffer. Approximately 1.5–2 $\times 10^4$ cells/cm^2 were seeded in 1.5 ml of synthetic medium. The cells were maintained initially for 30 min in supplemented minimum essential medium (MEM) plus Earle's salts (1:1) (composition: 2 mM glutamine, 600 mg/100 ml glucose, 20 units/ml penicillin, 20 µg /ml streptomycin), followed by conditioned medium for 4 h (composition: 80% MEM, 10% fetal calf serum, 10% heat-inactivated horse serum), followed by synthetic medium (composition: MEM and Ham's F-12 medium). The synthetic medium contained equal volumes of Ham's F-12 and DMEM supplemented with an additional 120 mg/100 ml glucose, 5 µg/ml bovine insulin, 100 µg/ml human transferrin, 20 nM progesterone, 100 µM putrescine, and 20 nM selenium dioxide. Penicillin and streptomycin were added to a final concentration of 20 units/ml and 20 µg/ml, respectively. The synthetic medium was used for long-term survival of the fetal stem cells. The culture was maintained in a humidified incubator with 5% CO$_2$ at 36°C. After 4–6 days, the division of nonneuronal cells was halted by the addition of 15 µg/ml fluorodeoxyuridine and 35 µg/ml uridine. These neuronal cultures could be maintained for 6–8 weeks. Cultured hippocampal and cerebellar neurons were used as nondopaminergic controls.

Neuronal culture

Human neuroblastoma (SK-N-SH) cell lines were cultured in DMEM, supplemented with high glucose, glutamine, 3.7 g/L sodium bicarbonate, and 10% fetal bovine serum (pH 7.4). The cells were incubated in a Forma Scientific CO$_2$ incubator set at 37°C with 5% CO$_2$ and 95% oxygen supply and humidified environment under aseptic conditions. The cells were grown in small T25 flasks to avoid contamination and were grown for 48 h in the above medium to subconfluent state. The cellular monolayer was detached using 0.25%

Trypsin-EDTA solution for 2 min at 37°C. Trypsin from detached cells was neutralized with 10% fetal bovine serum, and the cells were spun at 1,200 rpm for 5 min. The cell pellet was washed three times with d-PBS (pH 7.4) and stored in a −80°C freezer before analysis.

Preparation of mitochondrial genome knockout neurons

Mitochondrial genome knockout DA neurons were prepared by supplementing Dulbecco's modified Eagle's complete medium with 5 µg/L ethidium bromide. This treatment for 4–6 weeks selectively suppressed the mitochondrial genome (without affecting the nuclear genome), as confirmed by its absence using RT-PCR specific primer sets encoding complex-1 activity. Mitochondrial genome knockout (RhO$_{mgko}$) neurons mimicked a cellular model of aging and exhibited typical characteristics of genetic susceptibility and neurodegeneration in response to parkinsonian neurotoxins. We characterized these cells by estimating mitochondrial superoxide dismutase (SOD), catalase, and glutathione peroxidase, and then determined their proliferative potential. Under phase-contrast microscopy, these cells exhibited typical granular appearance due to mitochondrial membrane aggregation. By using fluorescence microscopy, we observed reduction in $\Delta\Psi$, perinuclear accumulation of MT, and α-Syn. The procedure to prepare aging RhO$_{mgko}$ cells is routinely performed and is well established in our lab. Although these cells can divide and afford neuroprotection in response to neuroprotective antioxidants, their bioenergetics are typically compromised and they exhibit genetic susceptibility to excitoneurotoxins and partial neuronal recovery in response to antioxidants. Transfection with mitochondrial genome, however, significantly improved their metabolic as well as their growth potential.

Lipid peroxidation

The cells were grown in 12-well plates for 72 h. Fresh medium was added to examine the effect of increasing concentrations of SIN-1, MT (100 nM), or selegiline (10 µM). The cells were harvested, suspended in d-PBS (pH 7.4), and sonicated at low wattage for 30 s, and then 1 ml of thiobarbituric acid reagent (composition: 15% trichloroacetic acid, 0.375% thiobarbituric acid, and 0.25 M hydrochloric acid) was added. The samples were heated for 20 min at 95°C, cooled in running ice-cold water, and then centrifuged at 10,000 rpm for 10 min. The optical density was measured at 535 nm spectral wavelength, using a microtiter plate reader. Bradford's reagent (Bio-Rad) was used to estimate the protein contents.

Radioimmunoprecipitation and immunoblotting

Radioimmunoprecipitation was performed by incubating the DA neurons in methionine-deficient DMEM, supplemented with 3.7 g/L sodium bicarbonate, 10% fetal bovine serum, and 1 µCi/ml [35S]methionine in the presence of SIN-1 (10 µM) and/or antioxidants (10 µM selegiline or 100 nM MT) overnight. The medium was removed, the cellular monolayer was washed three times with with dPBS (pH 7.4), and lysed in the lysis buffer containing Tris, EDTA, and dithio-

threitol. Specific monoclonal antibodies with recommended dilutions were added along with 100 µl of protein A-agarose. The samples were kept on a rotary shaker for 48 h at 4°C and centrifuged at 14,000 rpm for 20 min, and then the supernatant was removed. The immunoprecipitated proteins were reconstituted in 100 µl of lysis buffer and placed in scintillation vials containing 5 ml of scintillation fluid (Scintiverse-2). The samples were counted in ^{3}H window using Beckman–Coulter TriCarb 3100 liquid scintillation counter above background.

For immunoblotting, 10 µl of cell lysate was used for microplate protein determination using a Bio-Rad protein assay kit, in 1:4 dilutions of the concentrated dye and bovine serum albumin (ranging from 0.625 ng to 20 µg) as a standard. The microtiter plates were read using a microplate reader at 600 nm spectral wavelength. Cell lysates containing 15 µg of protein were subjected to 12% sodium dodecyl sulfate–polyacrylamide gel electrophoresis. Proteins were transferred onto nitrocellulose paper by electroblotting using 50 mA current strength for 1.5 h, and transfer efficiency was checked by Ponceau red stain. The blots were incubated overnight in 5% nonfat milk for nonspecific binding, washed three times in phosphate-buffered saline (pH 7.4), and subjected to 1:500 dilution of primary antibody to α-Syn for 1 h. Then the blots were washed three times with phosphate-buffered saline (pH 7.4) and exposed to 1:10,000 secondary antibody (horseradish peroxidase-labeled anti-mouse IgG) for 2 h. An Amersham chemiluminescent kit was used for developing the autoradiograms, which were quantitated using a Bio-Rad calibrated GS-800 densitometer.

HPLC and striatal microdialysis

HPLC was performed using an ISCO pump and JCL-6000 computer software equipped with Bioanalytical Systems electrochemical detector. Various monoamines and their metabolites, including norepinephrine, DA, dihydroxybenzoic acid, dihydroxyphenylacetaldehyde (DOPAL), homovanillic acid, 5-hydroxytryptamine, and 5-hydroxyindole-3-acetic acid were estimated prior to and following overnight exposure to SIN-1 (100 µ*M*), MT, or selegiline. The conversion rates of various monoamines to their metabolites were estimated quantitatively by using computer software and by preparing the overlay chromatograms before and after antioxidant treatment. The time-dependent accumulation of DOPAL was related directly to oxidation of DA. To correlate and confirm the SIN-1-induced DA oxidation *in vivo,* SK-N-SH neurons were incubated with SIN-1 and selegiline or other neuroprotective antioxidants, such as coenzyme Q_{10}, melatonin, or MT-1. For striatal microdialysis, the animals were anesthetized with tribromoethane (350 mg/kg, i.p). Microdialysis was performed by using Bioanalytical System, microdialysis probe, syringe pump, and refrigerated microcentrifuge. Artificial CSF, at a flow rate of 2 µl/min, was used to collect the microdialysates in 300 µl glass tubes. DA levels from the microdialysates were estimated by HPLC with electrochemical detection, and metal ions were determined by atomic absorption spectrometry. ATP levels were estimated using an ATP-Lite kit as per the manufacturer's instructions. Nitrotyrosine and 8-OH-2dG levels were estimated spectrofluorometrically by adding FITC-labeled antibodies to nitrotyrosine and 8-OH-2dG, respectively, using microtiter plates.

Cell transfection

The SK-N-SH neurons were transiently transfected using liposome-based Effectine reagent with DNA enhancer and transfection buffer using specific RT-PCR amplified gene products such as caspase-3 and mitochondrial genome. For stable transfection, pEGFP-N1 vector was used as per the manufacturer's recommendations. The reporter gene (green fluorescent protein) analysis was done using enrichment medium and real-time digital fluorescence imaging following selection with geneticin (G418) (250 µg/ml) for 4 weeks. The cells were selected using the limiting dilution technique and grown further to study the expression of caspase-3, as well as mitochondrial genome, using routine radioimmunoprecipitation, immunoblotting, and RT-PCR using specific primers. The control and transfected cells were used to study the influence of SIN-1 on DA synthesis, lipid peroxidation, and apoptosis using multiple fluorochrome analysis and ΔΨ.

RT-PCR

RT-PCR was performed using a Stratagene first-strand cDNA kit to prepare cDNA and by using a murine leukemia virus reverse transcriptase as per the manufacturer's instructions. Furthermore, caspase-3, mitochondrial genome encoding complex-1 region (ND-1), glyceraldehyde phosphate dehydrogenase (GAPDH), and MT genes were amplified using specific primer sequences (obtained from the Gene Bank) employing appropriate denaturing, annealing, and polymerization thermal cycle protocols. The genes were amplified using a Brinkmann-Eppendorf Gradient Thermal Cycler. The mRNA was reverse-transcribed using a murine leukemia virus reverse transcriptase. *Taq* DNA polymerase (2.5 U/0.5 µl) was used to amplify genes using specific primer sets and thermal cycles. The amplified products of different molecular weights were resolved simultaneously using 1% agarose gel (GibcoBRL) and visualized using a gel documentation system equipped with video camera, UV illuminator, and digital Sony printer. The amplified bands were semiquantitated using a calibrated Bio-Rad (GS-800) densitometer taking GAPDH as a housekeeping gene for normalizing the data.

Estimation of mitochondrial ions using atomic absorption spectrometry

DA neurons were treated with SIN-1 and/or selegiline or MT-1 overnight. The mitochondria were isolated and sonicated for 30 s at low wattage using 0.4 *M* perchloric acid. The mitochondrial homogenate was centrifuged at 14,000 rpm for 20 min at 4°C. The supernatant was passed through 2-nm syringe tip filters, and subjected to atomic absorption spectrophotometeric analysis to determine intramitochondrial free ionized copper, iron, zinc, and calcium. A graphite furnace operating in an argon environment was used to pyrolyze samples at 1,300–1,700°C and atomize at 2,200–2,800°C using optimal slit widths and spectral wavelengths for each element. Perkin Elmer (AA-Analyst) equipped with WinLab computer software was used for data analysis.

Caspase-3 activation and mitochondrial apoptosis

Caspase-3 activity was measured spectrofluorometrically using specific caspase-3 substrate AC-DEVD-AMC, and inhibitor AC-DEVD-CHO to ensure specificity. Mitochondrial apoptosis was determined by using the fluorochrome JC-1, as described.

Fluorescence microscopy and the neuroprotective potential of antioxidants

Striatal fetal stem cells from control$_{wt}$, MT$_{dko}$, and MT$_{trans}$ experimental genotypes were grown on glass cover slips or multichambered microscopic slides, maintained in DMEM, and supplemented with 10% fetal bovine serum. The cells were grown for 48 h to subconfluent stage, and were exposed to SIN-1 (10–250 μM), selegiline (10 μM), or MT-1 (100 nM) overnight. Following incubation, they were washed three times in d-PBS, and incubated at 37°C for 30 min to stain with the mitochondrial marker JC-1 (5 nM), and counterstained for 30 s in 10 µg/ml acridine orange. Acridine orange DAPI and/ or ethidium bromide DAPI preferentially stain structurally intact nuclear DNA, whereas ethidium bromide stains fragmented DNA. The cells were washed three times with d-PBS, mounted on microscopic slides using Aqua Mount supplemented with a photobleach inhibitor, and observed under a digital fluorescence microscope (Leeds Instruments Co., Minneapolis, MN, U.S.A.) set at three (blue for DAPI, green for acridine orange or FITC, and red for ethidium bromide or JC-1) spectral wavelengths. The fluorescence images were captured using a SpotLite digital camera and Image-Pro computer software. Target accentuation and background inhibition computer software were utilized to improve the quality of images. The images were merged to estimate mitochondrial versus nuclear apoptosis simultaneously.

Statistical analysis

Repeated measure analysis of variance (repeated ANOVA) was used for the statistical evaluation of the experimental data using Sigma-Stat (version 2.03). The numbers of observations made in each experimental group are presented in the figure legends. Values of $p < 0.05$ were considered statistically significant.

RESULTS

Radioimmunoprecipitation and immunoblotting

Overnight exposure of SIN-1 (100 nM) significantly ($p < 0.05$) inhibited Bcl-2 and poly(ADP-ribose) (PARP) and induced Bax, MT-1, and cytochrome C release, as demonstrated by radioimmunoprecipitation (Fig. 1A). Coincubation with
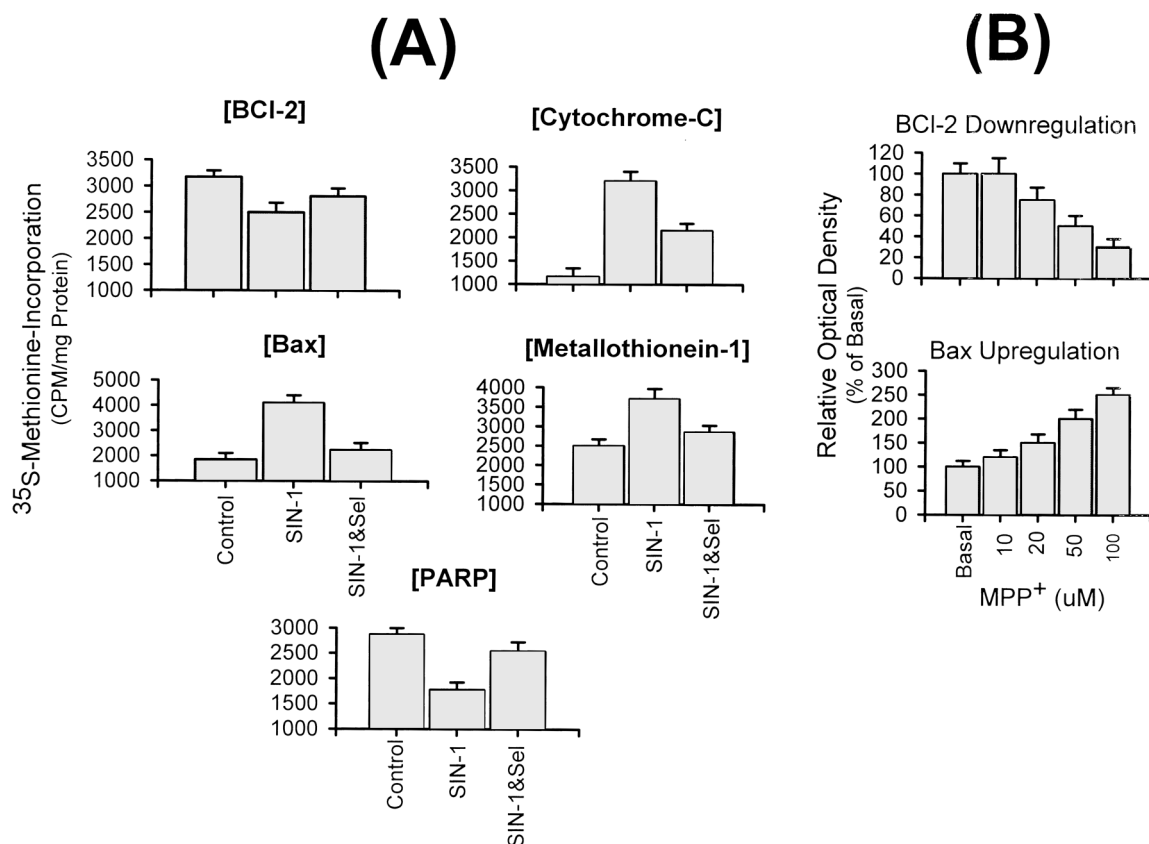

FIG. 1. (**A**) Quantitative analysis of Bcl-2, cytochrome C, Bax, MT-1, and PARP in response to overnight exposure of SIN-1 (1 µM) and/or selegiline (10 µM) in DA (SK-N-SH) neurons using radioimmunoprecipitation method. (**B**) Quantitative analysis of immunoblots demonstrating concentration-dependent down-regulation of Bcl-2 and up-regulation of Bax in response to overnight exposure to MPP⁺. Data are means ± SD of five determinations in each experimental group.

MT-inducer selegiline attenuated SIN-1-induced alterations in gene expression. A potent NOS activator, 1-methyl-4-phenylpyridinium ion (MPP+; 100 μM), induced concentration-dependent down-regulation of Bcl-2 and up-regulation of Bax as demonstrated by immunoblotting. A quantitative analysis of SIN-1-induced down-regulation of Bcl-2 and up-regulation of Bax is presented in Fig. 1B. MPP+ and 6-OHDA also significantly ($p < 0.01$) increased mitochondrial 8-OH-2dG synthesis and AIF release in a concentration-dependent manner in the DA (SK-N-SH) neurons. Coincubation with selegiline suppressed MPP+ and 6-OHDA-induced increases in AIF release (Fig. 2A). Various Lewy body molecular markers, including α-Syn, parkin, ubiquitin, caspase-3, 8-OH-2dG, and protein nitration, were induced upon overnight exposure of DA neurons to SIN-1 (100 nM). Coincubation with selegiline (10 μM) attenuated SIN-1-induced induction of the aforementioned Lewy body molecular markers (Fig. 2B).

Atomic absorption spectrometry

Intramitochondrial concentrations of various metal ions, including copper, iron, zinc, and calcium, were also significantly ($p < 0.05$) increased in response to overnight SIN-1 (100 nM) exposure. Coincubation with selegiline (10 μM) or MT-1 (100 nM) suppressed SIN-1-induced intramitochondrial accumulation of these ions (Fig. 3).

Striatal microdialysis

Using striatal microdialysis, we observed that an acute exposure of MPTP (30 mg/kg, i.p), which enhances brain regional NO, reduced the level of ATP, increased the concentration of nitrotyrosine, and augmented the release of 8-OH-2dG in the striatum (Fig. 4).

Lipid Peroxidation

To confirm the involvement of oxidative and nitrative stress during neurodegeneration, we conducted an *in vitro* analysis of SIN-1-induced lipid peroxidation in control$_{wt}$, caspase-3-transfected SK-N-SH, and aging RhO$_{mgko}$ neurons. Overnight exposure of DA (SK-N-SH) neurons to SIN-1 (100 nM) induced lipid peroxidation. SIN-1-induced lipid peroxidation was significantly ($p < 0.01$) enhanced in caspase-3-transfected and aging RhO$_{mgko}$ DA (SK-N-SH) neurons (Fig. 5A). Coincubation with selegiline significantly ($p < 0.01$) suppressed SIN-1-induced lipid peroxidation. Transfection of aging RhO$_{mgko}$ neurons with mitochondrial genome encoding
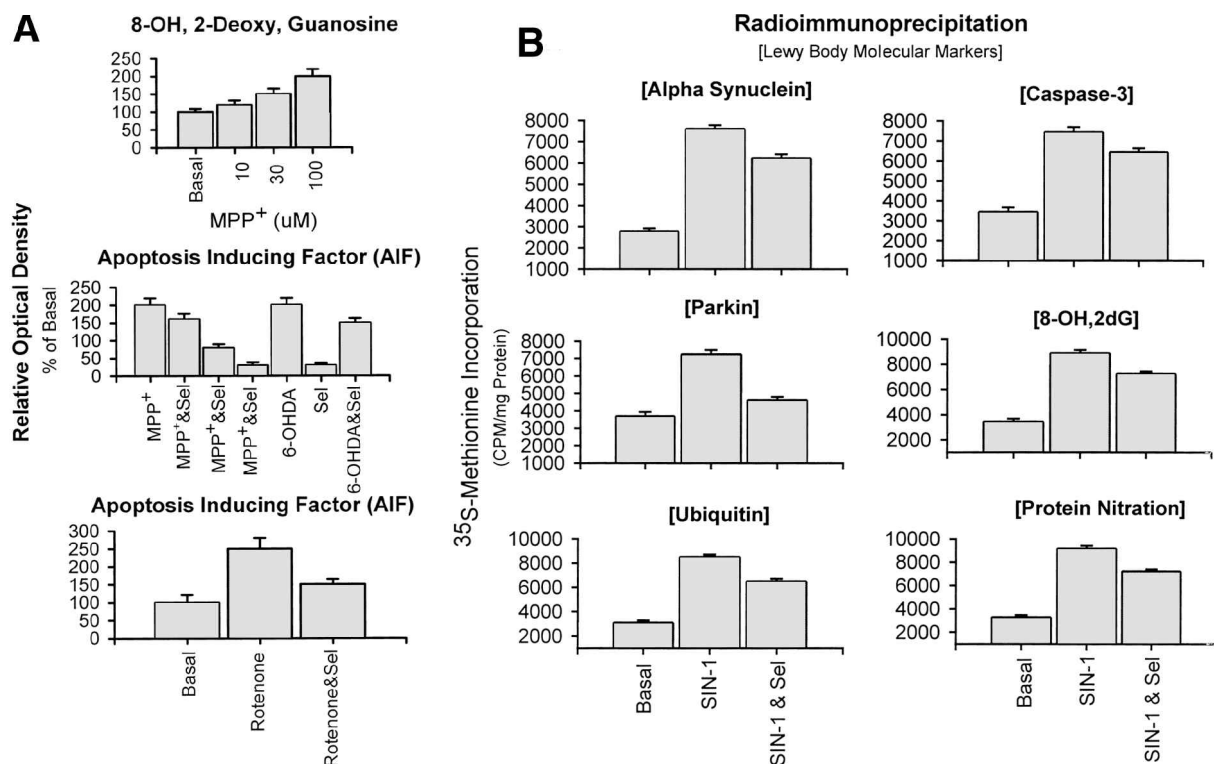

FIG. 2. (A) A quantitative analysis of immunoblots demonstrating MPP+ and 6-OHDA-induced increases in mitochondrial 8-OH-2dG synthesis and release of AIF in response to SIN-1, and their attenuation with selegiline coincubation in DA (SK-N-SH) neurons. (B) Histograms demonstrating significant ($p < 0.05$) induction of α-Syn, parkin, ubiquitin, caspase-3, 8-OH-2dG, and protein nitration in response to overnight exposure of SIN-1, and their attenuation upon coincubation with selegiline. Data are means ± SD of six to eight determinations in each experimental group (repeated measures ANOVA).
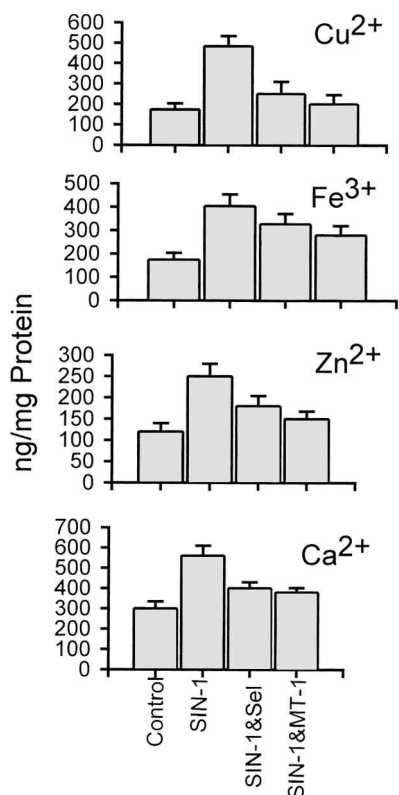
FIG. 3. Histograms demonstrating intramitochondrial accumulation of Cu^{2+}, Fe^{3+}, Zn^{2+}, and Ca^{2+} in response to overnight exposure of DA (SK-N-SH) neurons to SIN-1, and following coincubation with either selegiline (10 μM) or MT-1 (100 nM) as determined by atomic absorption spectrometry.

complex-1 activity significantly ($p < 0.01$) suppressed SIN-1-induced lipid peroxidation, as shown in Fig. 5A.

Melanin estimation

MT_{trans} mice possessed relatively higher levels of melanin in skin, hair, and SN as compared with $control_{wt}$ or MT_{dko} mice. The exact pathophysiological significance and clinical relevance of these findings remain enigmatic. Significantly higher levels of melanin in MT_{trans} mice could provide additional protection in these animals in response to parkinsonian neurotoxin neurotoxicity, as compared with MT_{dko} and $control_{wt}$ mice. SN melanin contents are also significantly reduced in aging PD patients (30), and subjects possessing reduced melanin are at high risk of developing PD during aging as compared with those possessing higher levels of melanin (58). In view of the above, we explored melanin-induced neuroprotection in SIN-1-exposed DA (SK-N-SH) neurons. Melanin suppressed SIN-1-induced lipid peroxidation in a concentration-dependent manner in the DA (SK-N-SH) neurons (Fig. 5B).

RT-PCR analysis of multiple genes

By using the RT-PCR procedure, we have analyzed multiple genes involved in parkinsonian neurotoxin-induced apop-

tosis and antioxidant (MT-1, selegiline, melatonin, coenzyme Q_{10})-induced antiapoptosis. Various genes involved in apoptosis (retinoic acid receptor, 1.3 kb; c-fos, 500 bp; c-jun, 350 bp; MT-1, 247 bp; and caspase-3, 200 bp) were significantly enhanced at the transcriptional level in response to overnight exposure to MPP^+ (100 μM), 6-OHDA (10 μM), rotenone (100 nM), salsolinol (100 μM), and SIN-1 (100 nM). Coincubation with antioxidant coenzyme Q_{10}, melatonin, and selegiline (10 μM each) significantly attenuated the transcriptional activation of these genes involved in apoptosis (Fig. 6A). SIN-1-induced transcriptional activation of apoptotic genes and down-regulation of antiapoptotic genes were attenuated upon MT-1 coincubation. Antiapoptotic genes [PARP, Bcl-2, and mitochondrial genome (complex-1)] were suppressed by SIN-1, whereas coincubation with antioxidants attenuated SIN-1-induced down-regulation of these genes. Overnight exposure of SK-N-SH neurons to rotenone (100 nM) also induced similar transcriptional down-regulation of antiapoptotic genes, which were up-regulated upon coincubation of cells with coenzyme Q_{10} (Fig. 6B). We have confirmed these observations using densitometric analysis and repeated measure ANOVA, as described in the figure legends.

Digital fluorescence imaging microscopy

To further confirm attenuation of SIN-1-induced apoptosis by MT-1, we used digital fluorescence imaging micro-
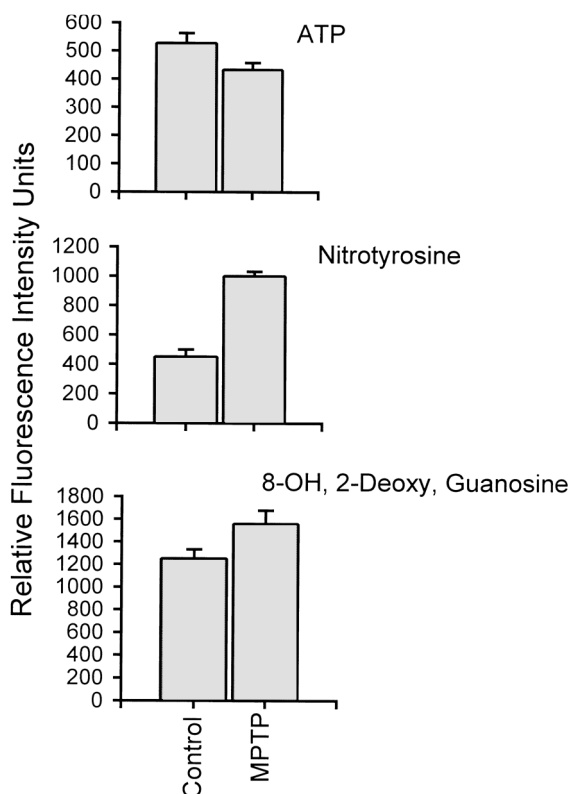

FIG. 4. Histograms demonstrating ATP, nitrotyrosine, and 8-OH-2dG release from the striatal microdialysates in response to acute MPTP (30 mg/kg, i.p.) treatment in mice. Microtiter spectrofluorometric determinations are presented.
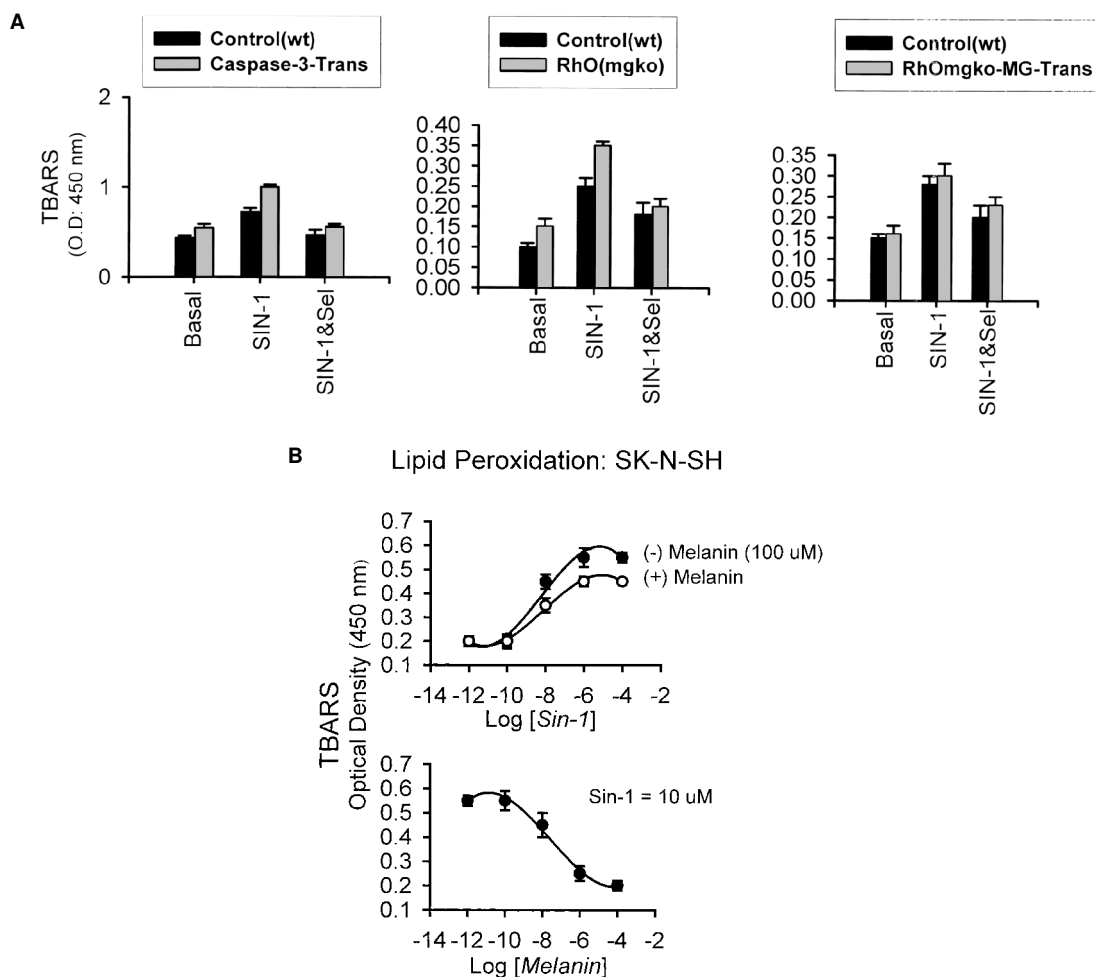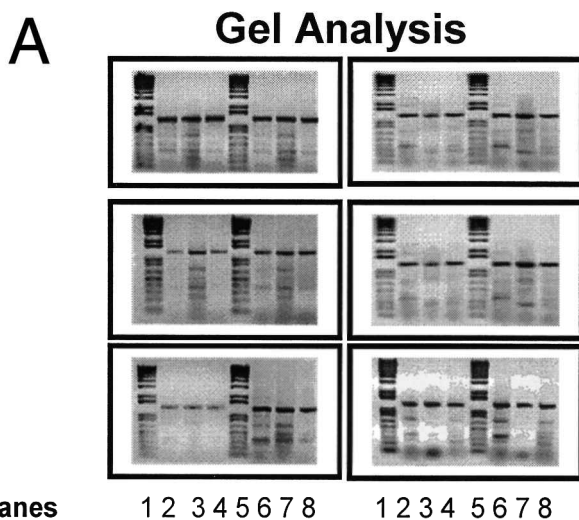
A

B

Lipid Peroxidation: SK-N-SH

FIG. 5. (**A**) Histograms representing SIN-1 (10 μM)-induced increase ($p < 0.01$) in lipid peroxidation in control$_{wt}$, caspase-3-transfected, and aging mitochondrial genome knockout (RhO$_{mgko}$) DA (SK-N-SH) neurons, and its suppression with either selegiline (10 μM) coincubation or transfection of RhO$_{mgko}$ neurons with mitochondrial genome encoding complex-1 (ubiquinone NADH oxidoreductase). Data are means ± SD of eight determinations in each experimental group (repeated measures ANOVA). TBARS, thiobarbituric acid reactive substances. (**B**) A concentration-dependent induction of lipid peroxidation in SK-N-SH neurons upon overnight SIN-1 exposure and its suppression by melanin coincubation.

FIG. 6. (**A**) RT-PCR analysis of multiple genes involved in apoptosis and antiapoptosis. **Upper left panel:** Lanes 1 and 5: molecular marker; 2 and 6: basal; 3: MPP+; 4: MPP+ + selegiline; 7: 6-OHDA; 8: 6-OHDA + selegiline. **Middle left panel:** Lanes 1 and 5: molecular marker; 2 and 6: basal; 3: salsolinol; 4: salsolinol + melatonin; 7: rotenone; 8: rotenone + melatonin. **Lower left panel:** Lanes 1 and 5: molecular marker; 2 and 6: basal; 3: SIN-1; 4: SIN-1 + ubiquinone; 7: rotenone; 8: rotenone + ubiquinone. Amplified genes from top: retinoic acid receptor (1.3 bp), c-fos (500 bp), c-jun (352 bp), and caspase-3 (200 bp). **Upper right panel:** Lanes 1 and 5: molecular marker; 2 and 6: basal; 3: MPP+; 4: MPP+ + selegiline; 7: 6-OHDA; 8: 6-OHDA + selegiline. **Middle right panel:** Lanes 1 and 5: molecular marker; 2 and 6: basal; 3: salsolinol; 4: salsolinol + melatonin; 7: rotenone; 8: rotenone + melatonin. Amplified genes from top: retinoic acid receptor (1.3 bp), α-Syn (500 bp), mitochondrial genome (complex-1: ubiquinone NADH oxidoreductase) (450 bp), metallothionein-1 (247 bp), and caspase-3 (200 bp). **Lower right panel:** Lanes 1 and 5: molecular marker; 2 and 6: basal; 3: SIN-1; 4: SIN-1 + ubiquinone; 7: rotenone; 8: rotenone + ubiquinone. Amplified genes from top: retinoic acid receptor (1.3 bp), PARP (800 bp), Bcl-2 (550 bp), mitochondrial genome (complex-1) (450 bp), and caspase-3 (200 bp). Densitometric analysis of amplified products was conducted by using calibrated Bio-Rad GS-800 densitometer equipped with Utility-1 software. SIN-1, MPP+, and 6-OHDA significantly ($p < 0.05$) enhanced c-fos, c-jun, caspase-3, and α-Syn expressions, and inhibited PARP, Bcl-2, and mitochondrial genome expressions. Selegiline pretreatment significantly ($p < 0.01$) attenuated SIN-1, MPP+, and 6-OHDA-induced changes in gene expression involved in apoptosis. Data are means ± SD of five determinations in each experimental group and were analyzed by using repeated measures ANOVA. Amplified gene product size in base pairs (bp) is presented in parentheses. (**B**) **Left panel:** RT-PCR analysis of multiple genes involved in rotenone-induced apoptosis and coenzyme Q$_{10}$-induced antiapoptosis. Rotenone (100 nM) inhibited PARP (800 bp), Bcl-2 (550 bp), mitochondrial genome encoding complex-1 (450 bp), and MT-1 (247 bp), whereas coenzyme Q$_{10}$ enhanced their expression. Lane 1: molecular marker; 2: basal; 3: rotenone; 4: rotenone + coenzyme Q$_{10}$. **Right panel:** Densitometric analysis of rotenone-induced enhanced expression of c-fos, c-jun, and caspase-3 genes and their suppression with coenzyme Q$_{10}$ pretreatment. The data are means ± SD of eight determinations in each experimental group and were normalized with the housekeeping GAPDH gene (452 bp; not shown).

scopy of striatal fetal stem cells derived from control$_{wt}$ and MT$_{trans}$ fetuses. SIN-1-induced apoptosis was characterized by plasma membrane perforations, nuclear DNA fragmentation, and condensation. SIN-1-induced apoptosis in control$_{wt}$ and MT$_{trans}$ striatal fetal stem cells is presented in Fig. 7. MT$_{trans}$ fetal stem cells exhibited genetic resistance to SIN-1-induced apoptosis, characterized by significantly reduced lipid peroxidation, membrane perforations, DNA fragmentation, and condensation. Overnight exposure of striatal fetal stem cells to SIN-1 (100 nM) induced oxidation of DA to DOPAL,

which was purified by using HPLC with electrochemical detection. DOPAL (10 μM)-exaggerated apoptosis was characterized by membrane perforations, nuclear DNA fragmentation, and condensation. MT$_{trans}$ striatal fetal stem cells exhibited inherent resistance to DOPAL-induced apoptosis, characterized by well preserved dendritic processes and suppressed mitochondrial and nuclear DNA fragmentation and condensation (Fig. 8). DOPAL-induced apoptosis was characterized by perinuclear aggregation of mitochondria and endonuclear induction and accumulation of MT-1. These apop-
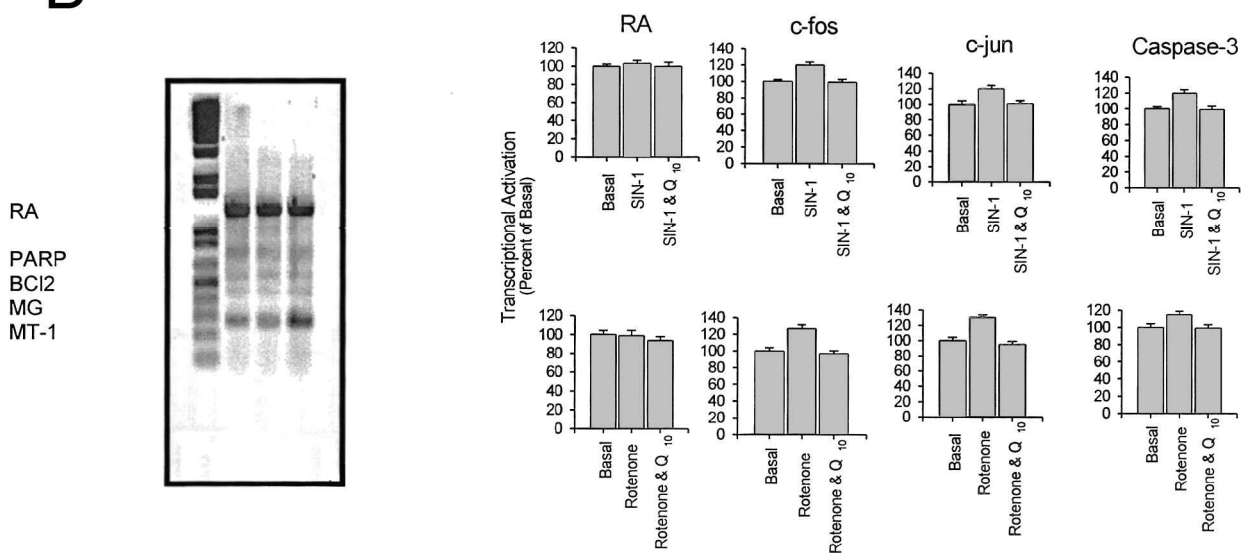
Multiple Genes: RT-PCR

A **Gel Analysis**

Lanes   1 2 3 4 5 6 7 8   1 2 3 4 5 6 7 8

Gel Analysis

Densitometric Analysis

B

RA
PARP
BCl2
MG
MT-1

RA   c-fos   c-jun   Caspase-3

Basal SIN-1 SIN-1 & Q$_{10}$

Basal Rotenone Rotenone & Q$_{10}$

Transcriptional Activation (Percent of Basal)

Coenzyme Q$_{10}$ (Ubiquinone) suppressed the transcriptional activation of apoptotic genes

Lanes   1 2 3 4

totic changes were significantly suppressed in MT_{trans} striatal fetal stem cells as compared with $control_{wt}$ cells.

DISCUSSION

The present study was conducted with a primary objective to explore the basic molecular mechanisms of neuroprotection afforded by MT. We have now demonstrated that SIN-1-induced nitrative as well as oxidative stresses can be attenuated in DA neurons by MT gene induction *in vitro* as well as *in vivo*. SIN-1 induced DA oxidation, lipid peroxidation, Bax up-regulation, and Bcl-2 down-regulation. Furthermore, DNA fragmentation was exaggerated in aging RhO_{mgko}, MT_{dko}, and caspase-3-transfected DA neurons. These changes were attenuated in MT_{trans}, MT-1, and mitochondrial genome-transfected DA neurons. SIN-1-induced neurodegenerative changes were also suppressed by exogenous administration of selegiline, melatonin, or coenzyme Q_{10}. SIN-1 enhanced α-Syn expression (molecular markers of Lewy body) and induced genes involved in apoptosis. Furthermore, pretreatment with antioxidants or MT-1 induction suppressed intramitochondrial as well as intranuclear biosynthesis of 8-OH-2dG, and intranuclear translocation of caspase-3, affording neuroprotection. These observations further confirm the possible beneficial effect of MT-1 induction in the treatment of PD.

By using RT-PCR and digital fluorescence imaging microscopy, we have now established that SIN-1 down-regulated mitochondrial genome encoding complex-1 activity, whereas pretreatment with either selegiline or MT suppressed this neurotoxicity.

The exact molecular mechanism of SIN-1-induced neurodegeneration remains unknown. It has been reported that NO can react with molecular oxygen (O_2), superoxide (O_2^-), and transition metals to produce nitrogen dioxide (NO_2), $ONOO^-$ ions, and metal nitrosyl adducts respectively, which might have pathological consequences (51). $ONOO^-$ ions have been implicated in progressive neurodegeneration in stroke, ischemia, Alzheimer's disease, PD, multiple sclerosis, motor neuron disease, and inflammatory diseases (3). O_2^- ions, produced by the reduction of O_2, have one unpaired electron that can

rapidly combine with the unpaired electron of NO to form $ONOO^-$. O_2^- levels are kept low by SOD, which dismutases O_2^- to H_2O_2 and catalyzes the dismutation reaction of O_2^-. However, in the presence of H_2O_2, SOD can produce potentially damaging $\cdot OH$ radicals and high levels of SOD can be damaging to the cell (7). Similarly, $ONOO^-$ has been implicated in various neuropathological processes (4). Nitration of protein tyrosine residues and neurofilaments is a convenient marker of $ONOO^-$ production and is enhanced by SOD overproduction (2). $ONOO^-$ can also inhibit the mitochondrial electron transport chain (41). Therefore, the overexpression of mitochondrial genome or MT-1 gene in aging RhO_{mgko} neurons attenuates SIN-1-induced lipid peroxidation and caspase-3 activation, suggesting the neuroprotective potential of MT gene overexpression.

Exogenous administration of MPTP enhances NOS activity as well as NO production in the SN, whereas NOS knockout animals exhibited neuroprotection against MPTP neurotoxicity (57), indicating the involvement of oxidative and nitrative stress in the etiopathogenesis of PD. Studies from our lab have established the neuroprotective and antioxidant role of MT in PD (12, 13). MT-1 mRNA expression was enhanced in response to acute 6-OHDA exposure (30), whereas chronic treatment with MPP^+ suppressed MT-1 mRNA expression in the rat striatum (44, 45). This further confirms the neuroprotective role of MT and the involvement of free radical-induced oxidative stress in the etiopathogenesis of PD.

It has been reported that $(-)$-deprenyl (selegiline) protects human DA neuroblastoma SH-SY-5Y cells from apoptosis via inhibition of $ONOO^-$ and NO (35, 39). ONOO-induced DNA fragmentation was also attenuated by *in vitro* administration of MT (36). Selegiline could produce neuroprotection through several possible molecular mechanisms. Our studies have now demonstrated that selegiline-induced neuroprotection of DA neurons is mediated through MT gene induction. In addition to its role as a potent monoamine oxidase B inhibitor, selegiline, as well as MT, can afford neuroprotection by acting as a modulator of cytokine expression. Both selegiline and MT trigger the DNA cell cycle and enhance cell proliferation and differentiation, as these agents are also involved in the growth and maintenance of brain regional cerebral DA neuro-

FIG. 7. A triple fluorochrome analysis of SIN-1-induced apoptosis illustrating genetic resistance of MT_{trans} as compared with $control_{wt}$ striatal fetal stem cells. The apoptotic cells exhibited rounded appearance with reduced neuritogenesis as observed in $control_{wt}$ as compared with MT_{trans} fetal stem cells. Triple fluorochrome analysis of apoptosis was performed using ethidium bromide, DAPI, and acridine orange. DAPI stained primarily intact nuclear DNA, ethidium bromide stained fragmented DNA, and acridine orange stained membrane proteins and RNA. Fluorescence images were captured after 24 h of exposure to SIN-1 (100 μM), using a SpotLite digital camera and ImagePro computer software. The images were merged to obtain detailed information about apoptosis as described in the text. (Note: $Control_{wt}$ cells exhibit typical membrane perforations, nuclear DNA fragmentation, and condensation in response to SIN-1.) Triple fluorochromes, acridine orange (green), ethidium bromide (red), and DAPI (blue), were merged to demonstrate SIN-1-induced membrane perforations, DNA condensation, and DNA fragmentation simultaneously. Magnification: $1,200\times$.

FIG. 8. Digital fluorescence images demonstrating resistance to DOPAL-induced apoptosis in MT_{trans} as compared with $control_{wt}$ striatal fetal stem cells within 24 h. DOPAL induced lipid peroxidation, membrane perforations, and DNA condensation and fragmentation particularly in $control_{wt}$ cells. Fluorescence images were captured with SpotLite digital camera and digitized using ImagePro computer software. Fluorochrome JC-1 (red) was used as a mitochondrial marker, and FITC-conjugated MT-1 (green) was used to obtain the structural and functional relationship between mitochondrial membrane potential and MT-1 expression. Fluorescence images were merged (**left panels**) to obtain overall information about perinuclear accumulation of mitochondria, as well as membrane perforations in response to DOPAL (**right panels**).
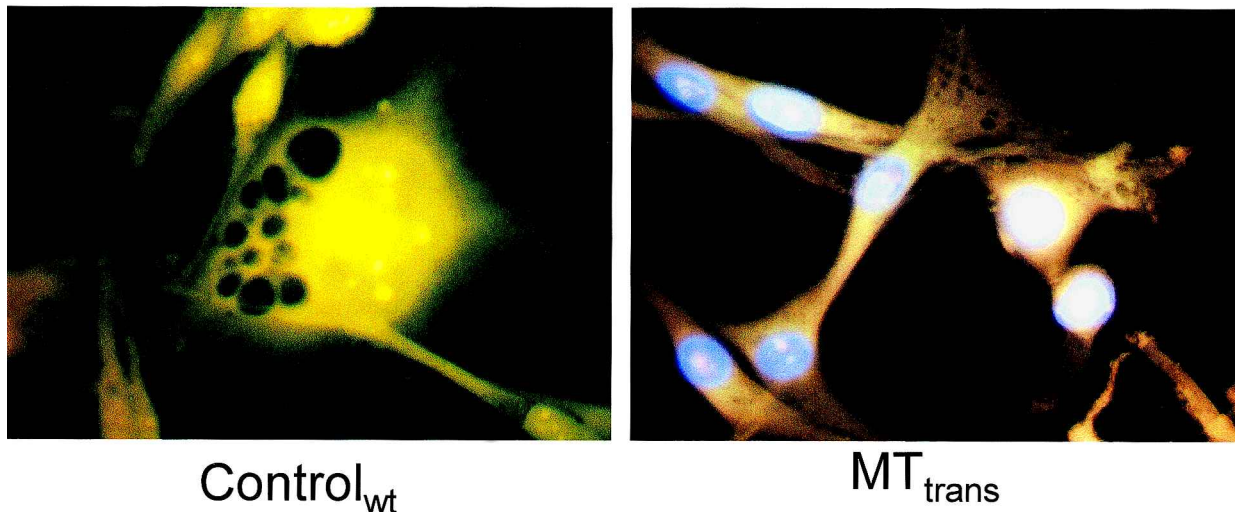
SIN-1-Induced Apoptosis

Control_{wt}   MT_{trans}

FIG. 7

DOPAL-INDUCED APOPTOSIS

[Striatal Fetal Stem Cells]   **DOPAL: 10 uM**

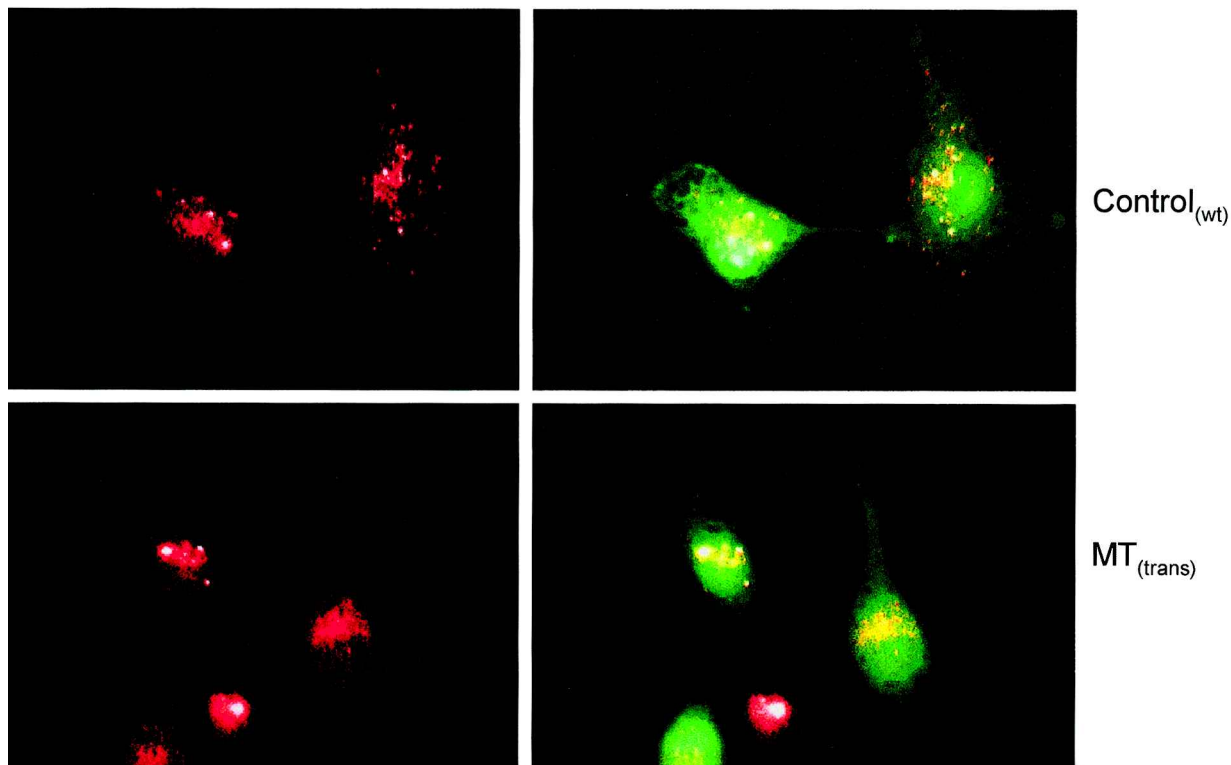Control_{(wt)}

MT_{(trans)}

FIG. 8

transmission. Indeed, by using brain regional microdialysis, we observed enhanced release of striatal DA from the MT_{trans}, as compared with MT_{dko} mice. We have now established that oxidation of DA to DOPAL, a potent neurotoxin, by SIN-1 is suppressed either by MT gene overexpression or in MT_{trans} fetal stem cells. SIN-1-induced DOPAL synthesis from DA oxidation was suppressed by MT gene induction, suggesting the neuroprotective potential of antioxidants in PD. In fact, the DA oxidation product DOPAL in PD suppresses brain regional DA neurotransmission and confirms the involvement of oxidative and nitrative stress in progressive neurodegeneration (27–29, 33, 36). Hence, treatment with antioxidant or brain regional overexpression of MT gene in the nigrostriatal region would have a beneficial effect in PD. Our studies have provided evidence that SIN-1-induced enhanced α-Syn expression and intramitochondrial accumulation of metal ions involved in the etiopathogenesis of PD are attenuated by pretreatment with MT or selegiline. These observations further authenticate the neuroprotective potential of MT induction in the treatment of PD.

The molecular mechanism of NO-mediated neurodegeneration in PD remains unknown. NO interacts with 6-OHDA to induce neurodegeneration via enhanced ·OH radical production (42). NO also enhances MPP^+-induced ·OH radical generation via activation of NOS in the rat striatum (38). Similarly, MPTP induces DA neurotoxicity through induction of iNOS (39). Thus, NO regulates monoaminergic neurotransmission in DA neurons (26). $ONOO^-$- and nitrite-induced oxidation of DA causes loss of DA cells in PD (31), whereas inhibition of neuronal NOS prevents MPTP-induced parkinsonism in baboons (19). Furthermore, iNOS knockout mice exhibited genetic resistance to MPTP neurotoxicity (18), whereas iNOS induced inflammation-induced DA neurodegeneration (23). $ONOO^-$ ions also inhibited DOPAL synthesis in PC12 cells (24), whereas a selective neuronal NOS inhibitor, 7-nitroindazole, protected mice against methamphetamine (25) and MPTP-induced neurotoxicity (46). In culture, MPP^+ increased the vulnerability to oxidative stress in human neuroblastoma (SH-SY-5Y) cells (32). NO-induced neurotoxicity was mediated through iNOS-mediated neurodegeneration of DA neurons in the MPTP model of PD (34). Significantly elevated levels of nitrites in the CSF would indicate the involvement of mitochondrial NOS activation and $ONOO^-$ generation in PD (40). MPTP-induced excessive NO production could also induce mitochondrial dysfunction in the DA neurons, as seen in PD (47).

Tetracyclines have been shown to slow down the progression of PD (11). Indeed, minocycline inhibits NO-induced phosphorylation of p38 mitogen-activated protein kinase (MAPK), whereas p38 MAPK inhibitor, SB203580, blocks NO toxicity, and blocks MPTP neurotoxicity by inhibiting $MPTP/MPP^+$-induced glial iNOS expression and by inhibiting the phosphorylation of p38 MAPK.

MPTP-induced neurotoxicity is associated with microglial iNOS induction, and hence the inhibition of iNOS may be a promising target for the treatment of PD (10). Indeed blockade of microglial cell activation fosters neuroprotection against the MPTP mouse model of PD (53). Similarly, a deficiency of iNOS protected against MPTP neurotoxicity (10). Following administration of MPTP to mice, there was a robust gliosis in the SN zona compacta, associated with signifi-

cant up-regulation of iNOS. These findings tend to suggest the involvement of microglial cell iNOS activation in the etiopathogenesis of PD.

In conclusion, the present study has demonstrated that the SIN-1-induced lipid peroxidation, α-Syn expression, intramitochondrial accumulation of metal ions, and apoptosis are suppressed in MT_{trans} fetal stem cells or MT-1 gene-overexpressed DA neurons, or by exogenous administration of antioxidants, such as selegiline. SIN-1 induced enhanced expression, as well as nitration, of α-Syn in aging RhO_{mgko}, caspase-3-overexpressed, and MT_{dko} mice. This was further substantiated by high levels of mitochondrial coenzyme Q_{10} in MT_{trans} mouse striatum as compared with that in MT_{dko} mice, which exhibited depletion of coenzyme Q_{10} following chronic MPTP treatment. This suggests the involvement of MT in neuroprotection against neurotoxic injury seen in PD. A further study using α-Syn-MT triple knockout mice on SIN-1 and MPTP is in progress; it will provide more insight regarding the intricate functional relationship between Lewy body molecular marker genes and apoptotic genes during neurodegeneration/regeneration and will go a long way in the clinical management of PD. Currently, selective monoamine oxidase A and B inhibitors, free radical scavengers, and NO inhibitors are being tried in the clinical management of PD, with limited success (54). The present study has provided novel evidence that MT gene overexpression could suppress $ONOO^-$-induced neurodegeneration in DA neurons, affording neuroprotection.

ACKNOWLEDGMENTS

ABBREVIATIONS

AIF, apoptosis-inducing factor; ANOVA, analysis of variance; $control_{wt}$, control wild type; DA, dopamine; DA neurons, dopaminergic neurons; DAPI, 4′,6-diamidino-2-phenylindole dihydrochloride; DMEM, Dulbecco's modified Eagle medium; DOPAL, dihydroxyphenylacetaldehyde; d-PBS, Dulbecco's phosphate-buffered saline; FITC, fluorescein isothiocyanate; GAPDH, glyceraldehyde phosphate dehydrogenase; HBSS, Hanks' balanced salt solution; iNOS, inducible nitric oxide synthase; JC-1, 5,5′,6,6′-tetrachloro-1,1′,3,3′-tetraethylbenzimidazolocarbocyanide iodide; MAPK, mitogen-activated protein kinase; MEM, minimum essential medium; MPP^+, 1-methyl-4-phenylpyridinium ion; MTP, 1-methyl-4-phenyl-1,2,3,6-tetrahydropyridine; MT, metallothionein; MT_{dko}, metallothionein double knockout; MT_{trans}, metallothionein transgenic; NO, nitric oxide; NOS, nitric oxide synthase; O_2^-, superoxide ion; ·OH, hydroxyl radical; 6-OHDA, 6-hydroxydopamine; 8-OH-2dG, 8-hydroxy-2-deoxyguanosine; $ONOO^-$, peroxynitrite; PARP, poly(ADP-ribose) polymerase; PD, Parkinson's disease; RhO_{mgko},

mitochondrial genome knockout; RT-PCR, reverse transcription–polymerase chain reaction; SIN-1, 3-morpholinosydnonimine; SN, substantia nigra; SOD, superoxide dismutase; α-Syn, α-Synuclein; ΔΨ, mitochondrial membrane potential.

REFERENCES

1. Beal MF. Excitotoxicity and nitric oxide in Parkinson's disease pathogenesis. *Ann Neurol* 44: S110–S114, 1998.

2. Beckman JS. Peroxynitrite versus hydroxy radical: the role of nitric oxide in superoxide-dependent cerebral injury. *Ann N Y Acad Sci* 738: 69–75, 1994.

3. Beckman JS and Koppenol WH. Nitric oxide, superoxide, and peroxynitrite: the good, the bad, and the ugly. *Am J Physiol* 271: C1424–C1437, 1996.

4. Beckman JS, Carson M, Smith CD, and Kopenol WH. ALS, SOD, and peroxynitrite. *Nature* 364: 584, 1993.

5. Bredt DS. Endogenous nitric oxide synthesis: biological functions and pathophysiology. *Free Radic Res* 31: 577–596, 1999.

6. Bringold U, Ghafourifar P, and Richter C. Peroxynitrite formed by mitochondrial NO synthase promotes mitochondrial Ca^{2+} release. *Free Radic Biol Med* 29: 343–348, 2000.

7. Brown RH. Amyotrophic lateral sclerosis. Recent insight from genetics and transgenic mice. *Cell* 80: 687–692, 1995.

8. Cai L, Klein JB, and Kang YJ. MT inhibits peroxynitrite-induced DNA and lipoprotein damage. *J Biol Chem* 275: 38957–38960, 2001.

9. Dawson VL and Dawson TM. Nitric oxide in neurodegeneration. *Prog Brain Res* 118: 215–229, 1998.

10. Dehmer T, Lindenau J, Haid S, Dichgans J, and Schulz JB. Deficiency of inducible nitric oxide synthase protects against MPTP toxicity in vivo. *J Neurochem* 74: 2213–2216, 2001.

11. Du Y, Ma Z, Lin S, Dodel RC, Gao F, Bales KR, Triarhou LC, Chernet E, Perry KW, Nelson DL, Luecke S, Phebus LA, Bymaster FP, and Paul SM. Minocycline prevents nigrostriatal DA neurodegeneration in the MPTP model of PD. *Proc Natl Acad Sci U S A* 98: 14669–14674, 2001.

12. Ebadi M, Pfeiffer RF, Murrin LC, and Shiraga H. Metallothionein and oxidation reactions in Parkinson's disease. *Proc West Pharmacol Soc* 34: 285–290, 1991.

13. Ebadi M, Leuschen MP, el Refaey H, Hamada FM, and Rojas P. The antioxidant properties of zinc and metallothionein. *Neurochem Int* 29: 159–166, 1996.

14. Ebadi M, Hiramatsu M, Burke WJ, Folks DG, and el-Sayed MA. MT isoforms provide neuroprotection against 6-hydroxy-dopamine-generated hydroxyl radicals and superoxide anions. *Proc West Pharmacol Soc* 41**:** 155–158, 1998.

15. Ebadi M, Govitrapong P, Sharma S, Muralikrishnan D, Shavali S, Pellett L, Schafer R, Albano C, and Eken J. Ubiquinone (coenzyme Q10) and mitochondria in oxidative stress of Parkinson's disease. *Biol Signals Recept* 10: 224–253, 2001.

16. Gerlach M, Blum-Degen D, Lan J, and Riederer P. Nitric oxide in the pathogenesis of Parkinson's disease. *Adv Neurol* 80: 239–245, 1999.

17. Ghafourifar P, Bringold U, Klein SD, and Richter C. Mitochondrial nitric oxide synthase, oxidative stress and apoptosis. *Biol Signals Recept* 10: 57–65, 2001.

18. Grunewald T and Beal MF. NOS knockouts and neuroprotection. *Nat Med* 5: 1354–1355, 1999.

19. Hantraye P, Brouillet E, Ferrante R, Palfi S, Dolan R, Matthews RT, and Beal MF. Inhibition of neuronal nitric oxide synthase prevents MPTP-induced parkinsonism in baboons. *Nat Med* 2: 1017–1021, 1996.

20. Hirsch EC and Hunot S. Nitric oxide, glial cells and neuronal degeneration in parkinsonism. *Trends Pharmacol Sci* 21: 163–165, 2000.

21. Hunot S, Dugas N, Faucheux B, Hartmann A, Tardieu M, Debre P, Agid Y, Dugas B, and Hirsch EC. FcepsilonRII/CD23 is expressed in Parkinson's disease and induces, in vitro, production of nitric oxide and tumor necrosis factor-alpha in glial cells. *J Neurosci* 19: 3440–3447, 1999.

22. Imam SZ, el-Yazal J, Newport GD, Itzhak Y, Cadet JL, Slikker W Jr, and Ali SF. Methamphetamine-induced dopamine neurotoxicity: role of peroxynitrite and neuroprotective role of antioxidants and peroxynitrite decomposition catalysts. *Ann N Y Acad Sci* 939: 366–380, 2002.

23. Iravani MM, Kashefi K, Mander P, Rose S, and Jenner P. Involvement of inducible nitric oxide synthase in inflammation-induced DA neurodegeneration. *Neuroscience* 110: 49–58, 2002.

24. Ischiropoulos H, Duran D, and Horwitz J. Peroxynitrite-mediated inhibition of DOPA synthesis in PC12 cells. *J Neurochem* 65: 2366–2372, 1995.

25. Itzhak Y and Ali SF. The neuronal nitric oxide synthase inhibitor, 7-nitroindazole, protects against methamphetamine-induced neurotoxicity in vivo. *J Neurochem* 67: 1770–1773, 1996.

26. Kiss JP. Role of nitric oxide in the regulation of monoaminergic neurotransmission. *Brain Res Bull* 52: 459–466, 2002.

27. Kristal BS, Conway AD, Brown AM, Jain JC, Ulluci PA, Li SW, and Burke WJ. Selective DA vulnerability: 3,4-dihydroxyphenylacetaldehyde targets mitochondria. *Free Radic Biol Med* 30: 924–931, 2001.

28. Lamensdorf I, Eisenhofer G, Harvey-White J, Hayakawa Y, Kirk K, and Kopin IJ. Metabolic stress in PC12 cells induces the formation of the endogenous dopamine neurotoxin, 3,4-dihydroxyphenylacetaldehyde. *J Neurosci Res* 60: 552–558, 2000.

29. Lamensdorf I, Eisenhofer G, Harvey-White J, Nechustan A, Kirk K, and Kopin IJ. 3,4-Dihydroxyphenylacetaldehyde potentiates the toxic effects of metabolic stress in PC12 cells. *Brain Res* 868: 191–201, 2000.

30. Lang AE and Lozano AM. Medical progress: Parkinson's disease. Parts 1 and 2. *N Engl J Med* 339: 1044–1053, 1130–1143, 1998.

31. LaVoie MJ and Hastings TG. Peroxynitrite- and nitrite-induced oxidation of dopamine: implications for nitric oxide in dopamine cell loss. *J Neurochem* 73: 2546–2554, 1999.

32. Lee HS, Park CW, and Kim YS. MPP(+) increases the vulnerability to oxidative stress rather than directly mediating oxidative damage in human neuroblastoma cells. *Exp Neurol* 165: 164–171, 2000.

33. Li SW, Lin T, Minteer S, and Burke WJ. 3,4-Dihydroxyphenylacetaldehyde and hydrogen peroxide generate a

hydroxyl radical: possible role in PD pathogenesis. *Brain Res Mol Brain Res* 93: 1–7, 2001.

34. Liberatore GT, Jackson-Lewis V, Vukosavic S, Mandir AS, Vila M, McAuliffe WG, Dawson VL, Dawson TM, and Przedborski S. Inducible nitric oxide synthase stimulates DA neurodegeneration in the MPTP model of Parkinson's disease. *Nat Med* 5: 1403–1409, 1999.

35. Maruyama W, Takahashi T, and Naoi M. (−)-Deprenyl protects human DA neuroblastoma SH-SY5Y cells from apoptosis induced by peroxynitrite and nitric oxide. *J Neurochem* 70: 2510–2515, 1998.

36. Mattammal MB, Haring JH, Chung HD, Raghu G, and Strong R. An endogenous DA neurotoxin: implication for Parkinson's disease. *Neurodegeneration* 4: 271–281, 1995.

37. Naoi M, Maruyama W, Yagi K, and Youdim M. Anti-apoptotic function of L-(−)deprenyl (Selegiline) and related compounds. *Neurobiology (Bp).* 8: 69–80, 2000.

38. Obata T and Yamanaka Y. Nitric oxide enhances MPP(+)-induced hydroxyl radical generation via depolarization activated nitric oxide synthase in rat striatum. *Brain Res* 902: 223–228, 2001.

39. Przedborski S, Jackson-Lewis V, Yokoyama R, Shibata T, Dawson VL, and Dawson TM. Role of neuronal nitric oxide in 1-methyl-4-phenyl-1,2,3,6-tetrahydropyridine (MPTP)-induced dopamine neurotoxicity. *Proc Natl Acad Sci U S A* 93: 4565–4571, 1996.

40. Qureshi GA, Baig S, Bednar I, Sodersten P, Forsberg G, and Siden A. Increased cerebrospinal fluid concentration of nitrite in Parkinson's disease. *Neuroreport* 6: 1642–1644, 1995.

41. Radi R, Rodriguez M, Castro L, and Telleri R. Inhibition of mitochondrial transport by peroxynitrite. *Arch Biochem Biophys* 308: 89–95, 1994.

42. Riobo NA, Schopfer FJ, Boveris AD, Cadenas E, and Poderoso JJ. The reaction of nitric oxide with 6-hydroxydopamine. Implications for Parkinson's disease. *Free Radic Biol Med* 32: 115–121, 2002.

43. Rojas P, Cerutis DR, Happe HK, Murrin LC, Hao R, Pfeiffer RF, and Ebadi M. 6-Hydroxydopamine-mediated induction of rat brain MT-I mRNA. *Neurotoxicology* 17: 323–334, 1996.

44. Rojas P, Hidalgo J, Ebadi M, and Rios C. Changes of MT-I+II proteins in the brain after 1-methyl-4-phenylpyridinium administration in mice. Prog *Neuropsychopharmacol Biol Psychiatry* 24: 143–154, 2001.

45. Rojas P, Rojas-Castaneda J, Vigueras RM, Habeebu SS, Rojas C, Rios C, and Ebadi M. MPTP decreases MT-I mRNA in mouse striatum. *Neurochem Res* 25: 503–509, 2001.

46. Schulz JB, Matthews RT, Muqit MM, Browne SE, and Beal MF. Inhibition of neuronal nitric oxide synthase by 7-nitroindazole protects against MPTP-induced neurotoxicity in mice. *J Neurochem* 64: 936–939, 1995.

47. Schulz JB, Matthews RT, Klockgether T, Dichgans J, and Beal MF. The role of mitochondrial dysfunction and neuronal nitric oxide in animal models of neurodegenerative diseases. *Mol Cell Biochem* 174: 193–197, 1997.

48. Sharma SK, Sangchot P, and Ebadi M. MT gene manipulation influences striatal mitochondrial ubiquinones and

MPTP-induced neurotoxicity in dopaminergic neurons. *World Congress of Pharmacology* 14: 106–107, 2002.

49. Sharma SK, Shavali S, EI Rafaey H, and Ebadi, M. Inhibition of α-Syn nitration and perinuclear aggregation by antioxidants in metallothionein transgenic and aging RhO (mgko) dopaminergic neurons. *FASEB J* 16: 686.11, 2002.

50. Smith KJ, Kapoor R, and Felts PA. Demyelination: the role of reactive oxygen and nitrogen species. *Brain Pathol* 9: 69–92, 1999.

51. Stamler JS, Singel DL, and Loscalzo J. Biochemistry of nitric oxide and its redox-activated forms. *Science* 258: 1898–1902, 1998.

52. Torreilles F, Salman-Tabcheh S, Guerin M, and Torreilles J. Neurodegenerative disorders: the role of peroxynitrite. *Brain Res Rev* 30: 153–163, 1999.

53. Wu DC, Jackson-Lewis V, Vila M, Tieu K, Teismann P, Vadseth C, Choi DK, Ischiropoulos H, and Przedborski S. Blockade of microglial activation is neuroprotective in the 1-methyl-4-phenyl-1,2,3,6-tetrahydropyridine mouse model of Parkinson's disease. *J Neurosci* 22: 1763–1771, 2002.

54. Youdim MB and Lavie L. Selective MAO-A and B inhibitors, radical scavengers and nitric oxide synthase inhibitors in Parkinson's disease. *Life Sci* 55: 2077–2082, 1994.

55. Youdim MB, Ben-Shachar D, Eshel G, Finberg JP, and Riederer P. The neurotoxicity of iron and nitric oxide. Relevance to the etiology of Parkinson's disease. *Adv Neurol* 60: 259–266, 1993.

56. Youdim MB, Lavie L, and Riederer P. Oxygen free radicals and neurodegeneration in Parkinson's disease: a role for nitric oxide. *Ann N Y Acad Sci* 738: 64–68, 1994.

57. Yun HY, Dawson VL, and Dawson TM. Nitric oxide in health and disease of the nervous system. *Mol Psychiatry* 2: 300–310, 1997.

58. Zecca L, Fariello P, Riederer P, Sulzer D, Gatti A, and Tampellini D. The absolute concentrations of nigral neuromelanin, assayed by a new sensitive method, increases throughout life and is dramatically decreased in Parkinson's disease. *FEBS Lett* 510: 216–220, 2002.

59. Zhang Y, Dawson VL, and Dawson TM. Oxidative stress and genetics in the pathogenesis of Parkinson's disease. *Neurobiol Dis* 7: 240–250, 2002.

Address reprint requests to:
Manuchair Ebadi, Ph.D., FACCP
Professor of Pharmacology, Physiology and Therapeutics
University of North Dakota School of Medicine
501 North Columbia Road
Grand Forks, ND 58203, U.S.A.

E-mail: mebadi@medicine.nodak.edu